

Polyvinyl Alcohol Food Packaging System Comprising Green Synthesized Silver Nanoparticles

Ahmed Elsayed Abdelhamid¹, Eman AboBakr Ali Yousif¹, Manal Mohamed Talaat El-Saidi², and Ahmed Ali El-Sayed^{2*}

¹Polymers & Pigments Department, National Research Centre, 33 El-Behouth St. Dokki, Cairo, Egypt

²Photochemistry Department, Chemical Research Division, National Research Center, Dokki, Giza, 12622, Egypt

* **Corresponding author:**

email: ahmedcheme4@yahoo.com

Received: April 18, 2020

Accepted: September 21, 2020

DOI: 10.22146/ijc.55483

Abstract: Green synthesis of silver nanoparticles (AgNPs) using aqueous *Moringa* extract and their incorporation in polyvinyl alcohol (PVA) as food packaging materials have been performed. The prepared nanoparticles were characterized via Ultraviolet-visible spectra and transmission electron microscope, and the results revealed the formation of silver nanoparticles in a semi-spherical shape with an average size ranged from 2 to 5 nm. The addition of different ratios of the nanoparticles onto the PVA matrix and their crosslinking via citric acid to obtain nanocomposite sheets were performed. The nanocomposite sheets were characterized using FT-IR, UV-Vis, and TGA. In addition, their mechanical properties were evaluated. Water vapor permeability rate and water content were also determined. The composite sheets showed good thermal and optical performance. Antibacterial activities of the prepared nanocomposite sheets were evaluated, and the results exhibited good resistance to bacterial growth.

Keywords: silver nanoparticles; green synthesis; polyvinyl alcohol; *Moringa* extract; food packaging

■ INTRODUCTION

As much of the world has placed concern on improving food safety, active packaging has gained the interest of many researchers. The addition of antioxidants and antibacterial components into packaging materials has proved its potential as an approach to increase the shelf life as well as preserve food nutrition quality [1-2]. Consequently, many attempts have been employed to develop an active packaging system containing bioactive compounds, essential oil, plant extracts, and nanomaterials [3]. The incorporation of nanotechnology helps increase not only the surface area for active components [4] but also the mechanical properties of packaging film [3]. With the development of nanomaterials, metal oxide nanoparticles show promising and far-ranging prospects for the biomedical field, especially for anti-bacteria, anticancer drug/gene delivery, cell imaging, bio-sensing, and so on [5-11]. Nano-silver is one of the predominant nano-metals that is well known for its efficiency as an antimicrobial agent and can be used in many applications

including packaging. There are many techniques for preparing metal nanoparticles to include chemical reduction, physical and biological methods [12-13]. On the whole, the green synthesis of metal nanoparticle preparation has been adapted as a good alternative to those that include microwave assessment or electrochemical reduction. Not only environmental awareness is the driving force for using biosynthesis of metal oxide, but also the low cost and efficiency of this technique. Biosynthesis of metal nanoparticles was implied by many researchers using microorganisms and plant leave [14], seed extract [15], or roots [13]. One of the considerable plants is *Moringa Oleifera*. It is a well-known plant grown not only in Asia but also in some other countries in Africa [16]. The rich content of natural compounds in its flowers, seeds, and leaf has made it an important ingredient in common and modern medicinal treatment. *Moringa* extract has extensively used in different application as anti-microbial, mosquito repellent, and food packaging [17-18].

There are many natural biodegradable polymers as chitosan and cellulose derivative have been employed for food packaging to preserve food safety as well as the environment vitality [19-20]. However, the low water resistance and sensitivity to the variation of pH lead to increasing interest in using synthetic biodegradable polymers. Polyvinyl alcohol (PVA) has characteristic chemical resistance combined with hydrophilic properties made it a promising candidate in food packaging [2,21-22]. Polyvinyl alcohol-based food packaging sheet was prepared using citric acid as crosslinking in the presence of grapefruit seed extract as an antimicrobial agent [23]. These polymeric sheets showed good water stability with weight loss of about 19% after 72 h immersion in water and good transparency with enhanced mechanical and antimicrobial performance. Novel biodegradable polyvinyl alcohol/starch/glycerol/halloysite nanotube nanocomposite films were prepared by solution casting technique [24]. The obtained films were characterized by excellent water resistance and good transparency to be potentially applied in food packaging, especially targeting lipophilic and acidic foodstuffs.

Although the utilization of Moringa extract for AgNPs synthesis has been reported previously, many researchers are still investigating the behavior of the Moringa extract/AgNPs combination. However, there are limited reports that introduce AgNPs in a final product form. In this work, a biodegradable composite sheet was prepared by combining biosynthesized silver nanoparticles (AgNPs with unique particle size) with PVA to produce active packaging. Biosynthesis of Ag nanoparticles using an aqueous *Moringa Oleifera* (MO) leaves extract, which was grown in Egypt, was carried out. After that, the AgNPs/MO suspension was added to the PVA solution with different amounts in the presence of citric acid as a crosslinking. The antimicrobial as well as the physical and mechanical properties of the prepared sheets were investigated.

■ EXPERIMENTAL SECTION

Materials

Polyvinyl alcohol (PVA) (M.Wt:78000) was purchased from Aldrich. *Moringa Oleifera* leaves were delivered from the Egyptian Scientific Society of Moringa

(ESSM), National Research Centre, Dokki, Cairo, Egypt, washed to remove any adhered contamination, dried, and ground. Silver nitrate (AgNO_3), citric acid, and sulfuric acid were delivered from Aldrich.

Procedure

Synthesis of Moringa leaves extract and in-situ nanoparticles production

Dry Moringa leaves (20 g) have been ground using a mortar. The resulted powder was suspended in distilled water (100 mL), heated at 60 °C under stirring for 1 h. The formed extract was then filtered. The Moringa extract (filtrate, 10 mL) was diluted with (90 mL) of deionized water in another conical flask. Silver nitrate (AgNO_3 , 0.17 g, 0.1 mmol) was added to this extract, with continuous stirring at 60 °C for 1 h, in which the in-situ silver formation takes place. The change to the brownish color of the resulting solution is an indication of the formation of silver nanoparticles, the nanoparticles formation was also confirmed and characterized by UV-Vis Spectrophotometer and TEM [25].

Preparation of PVA-AgNPs nanocomposite sheets

The PVA/AgNPs/MO nanocomposite sheets were prepared by adding different volumes (2.5 and 10 mL) of AgNPs/MO suspensions to 25 mL of PVA containing 1 g polymer content that dissolved in distilled water at 90 °C under stirring. After the addition of the nanoparticles, they were stirred for a while and sonicated by a water bath sonicator for 30 min. The citric acid (0.125 g) was added to the polymer solution as a crosslinking agent with the addition of a few drops of sulfuric acid as a catalyst for the esterification process. The mixture was stirred for about 2 h at 70 °C; after that, it was poured into a petri- dish and then left to be dried in an oven at 50 °C for 2 days to obtain PVA-Ag (2.5) and PVA-Ag (10). Blank un-crosslinked PVA (that prepared without citric acid) and crosslinked (CPVA) were also prepared for comparison.

Characterization of nanoparticles and nanocomposite films

Ultraviolet-visible spectroscopy (UV-Vis). AgNPs formation by Moringa leaves extract was monitored using a Jenway UV/Vis spectrophotometer (Jenway

UV/Visible-2605 spectrophotometer, England). The transparency of PVA sheets was evaluated using UV-Vis spectra in the visible range between 400–700 nm.

Transmission electron microscope (TEM). Evaluation of the size and shape of AgNPs was performed using High-Resolution Transmission Electron Microscopy (HR-TEM) JEOL (JEM-2100 TEM). A drop of colloidal solution was placed on a copper grid and was left in the air at room temperature to evaporate the solvent.

FTIR spectroscopy. The functional groups of the nanocomposite PVA films were confirmed using Fourier Transform Infrared (FTIR) (Shimadzu 8400, Japan) spectrophotometer in the spectral range between 400 and 4000 cm^{-1} .

Thermal gravimetric analysis (TGA). Thermal analysis of the prepared samples was achieved using a Shimadzu Instrument. The measurements were carried out with a heating rate of 10 $^{\circ}\text{C}/\text{min}$ within the range of 0 to 400 $^{\circ}\text{C}$ in a nitrogen atmosphere.

Mechanical properties

The mechanical performance (tensile strength and elongation at break) for PVA nanocomposite films containing different ratios of nanoparticles was tested using Zwick/Roell Z010, type Xforce P, S/N: 760608, Germany. The film samples were cut into a dumbbell shape, and the measurements were tested at a crosshead speed of 2 mm/min at 25 $^{\circ}\text{C}$.

Water content

For water content determination, the films ($1.5 \times 1.5 \text{ cm}^2$) were cut and soaked in distilled water for about 24 h, then weighed (W_s) and dried in the oven at 80 $^{\circ}\text{C}$ until a constant weight (W_d) was achieved. The average data of three replicate measurements were used to calculate the water content by applying the following equation:

$$\text{Water content} = \frac{W_s - W_d}{W_s} \times 100 \quad (1)$$

Water vapor permeation rate

For investigating water vapor permeability, a certain volume of distilled water was introduced into vials; then, the vials were mounted tightly with nano-composite film samples with the aid of certain tape and weighted. The vials weight was measured at an interval time, and the

water vapor permeability rate was calculated using the following equation:

$$\text{WVPR} = \frac{k}{A} \quad (2)$$

where k is rate constant can be estimated from the slope of the regression line of the plot of weight differences versus time, and A is the surface area of the sheet [26].

Antibacterial assay

The antibacterial performance of blank PVA and composite sheets against *Escherichia coli* (*E. coli*) as Gram-negative and *Staphylococcus aureus* (*S. aureus*) as Gram-positive bacterial strains, respectively, were examined as reported previously [27]. Agar diffusion plate test was used to explore the antibacterial action; the bacteria strains were cultivated on agar comprises nutrient and incubated for 24 h at 37 $^{\circ}\text{C}$. A hundred μL of diluted bacterial suspension was spread onto the Petri dish, and the test sample disks were fixed on the surface of the agar. These samples were incubated at 37 $^{\circ}\text{C}$ for a day. After incubation, the inhibition zone area was evaluated [28].

RESULTS AND DISCUSSION

Moringa Leaves Extract and in-situ Nanoparticles Preparation

The phytochemical examination of Moringa extract confirms the presence of a variety of unique compounds. This plant category is rich in phenolic compounds that include glucosinolates, a simple sugar, isothiocyanates, and rhamnose [29-30]. It has been found that Moringa extract has appropriate reducing and stabilizing potency during the preparation of AgNPs. The reduction of Ag^+ cation into Ag^0 has been carried out by the glucosinolates and sugar to form and stabilize AgNPs; meanwhile, the glucosinolates have been oxidized to gluconic acid [31]. The reduction of silver cation can also be made by some organic compounds that have reductive groups such as $-\text{OH}$, $-\text{SH}$, $-\text{NH}$, etc. Fig. 1 shows some examples of the organic compounds selected phytochemicals from Moringa as reported in the literature [32]. The preparation of AgNPs from Ag^+ using MO leaves s extract has been followed by the color change of the reaction.

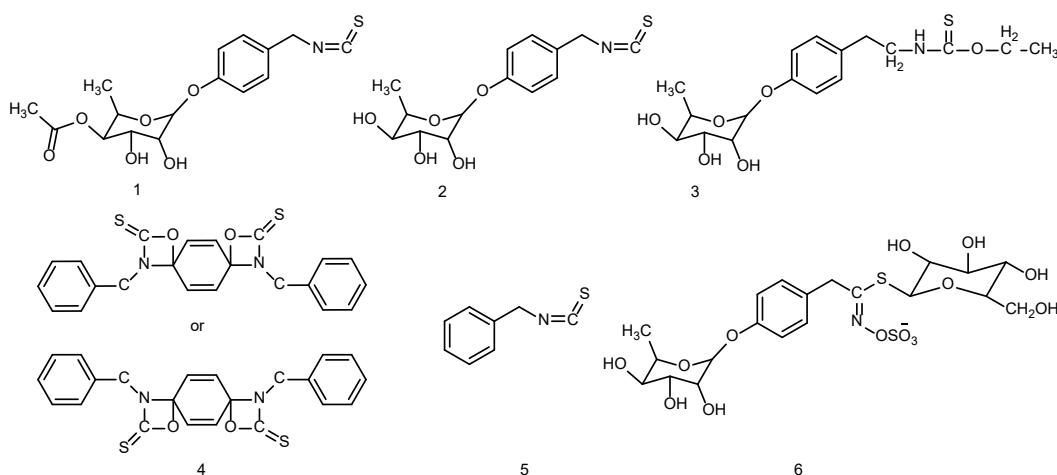


Fig 1. Common compounds of MO extract

Ultraviolet-Visible Spectroscopy (UV-Vis)

The change of color of the Moringa extract to brown one was the first confirmation of the biosynthesis of Ag nanoparticles. Fig. 2 represents another confirmation of AgNPs/MO preparation via the appearance of the characteristic peak in the range of 300–480 nm [25], whereas the peak that appeared at 340 nm may be attributed to the resultant nanoparticles extract suspension. The UV spectra were displayed as combined peaks in the region between 300 and 400 nm that may be due to the high optical density of the solution [33]. Moringa extract is rich with flavonoids and phenolic compounds and thereby helped in preventing aggregation by electrostatic stabilization; also, certain bio-organics presented in the Moringa extract may have brought about electro-steric stabilization [24].

Transmission Electron Microscopy (TEM)

The TEM image of the prepared nanoparticles is shown in Fig. 3. A semi-spherical shape of AgNPs/MO with a unique particle size was successfully obtained. It also reveals a homogenous size of AgNPs/MO with a mean average size of 3.1 ± 0.02 nm width. The histogram chart showed that the size of AgNPs/MO lies in the range between 2 and 5 nm. It was reported that increasing the concentration of MO extract leads to a reduction of particle size [24]. However, in this work, this extraordinary particle size may be attributed to the MO extract richness of phenols, flavonoids, and bioactive compounds. Even the TEM image gives homogenous particle size with no obvious aggregations, the AgNPs/MO suspension may contain some aggregate, and this was assessed by the presence of surface plasmon

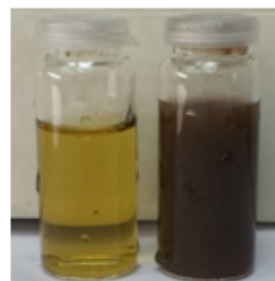
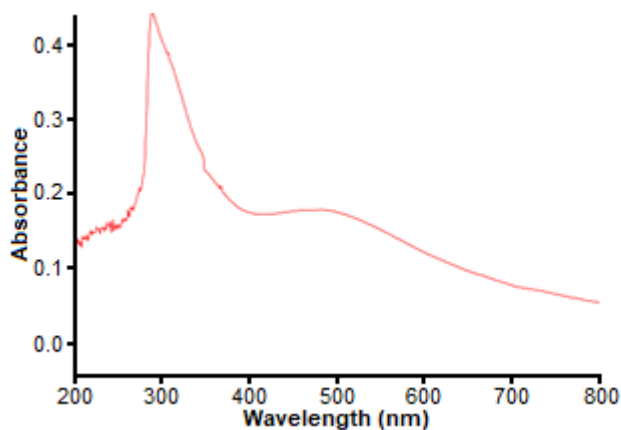


Fig 2. (a) UV-spectra of biosynthesized AgNPs and (b) digital photo for Moringa extract and Moringa/AgNPs

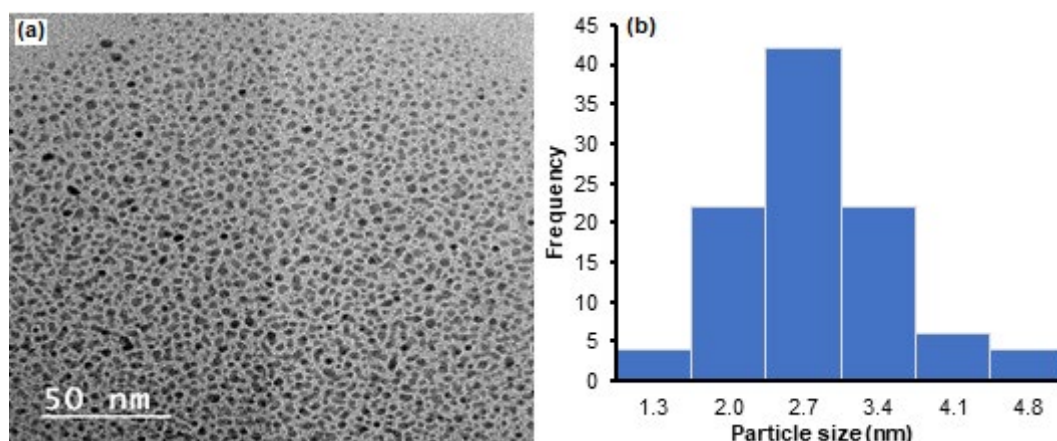


Fig 3. TEM images (a) and histogram (b) of biosynthesized AgNPs Moringa leaves extract

resonance in UV-vis in the region of 455–800 nm [24].

IR Analysis

Fig. 4 shows the change of the chemical structure upon the modification of PVA. The broad band in the range of 3429 cm^{-1} represents the richness of OH groups in pure PVA chains, and the peaks of CH_2 and CH were clearly seen at 2900 and 2854 cm^{-1} , respectively [34–35]. The absorption at 1070 cm^{-1} is related to the C–O stretching vibration of primary alcohol [36]. The absorption at 1720 cm^{-1} is corresponding to the stretching of the carbonyl group of citrate ester. After the addition of

AgNPs/MO, a new peak was observed at 548 cm^{-1} which attributed to silver nanoparticles, and the peak at 1070 cm^{-1} was greatly reduced, which may be involving the OH groups in the reduction or stabilizing silver nanoparticles. There are a small shift of the CH_2 peak from 2900 to 2926 cm^{-1} and the broadening of the OH band around 3429 cm^{-1} which may be due to the formation of hydrogen bonding between OH of PVA and the active compound in MO extract. All these results indicate the successful incorporation of AGNPs/Mo within the PVA polymer matrix.

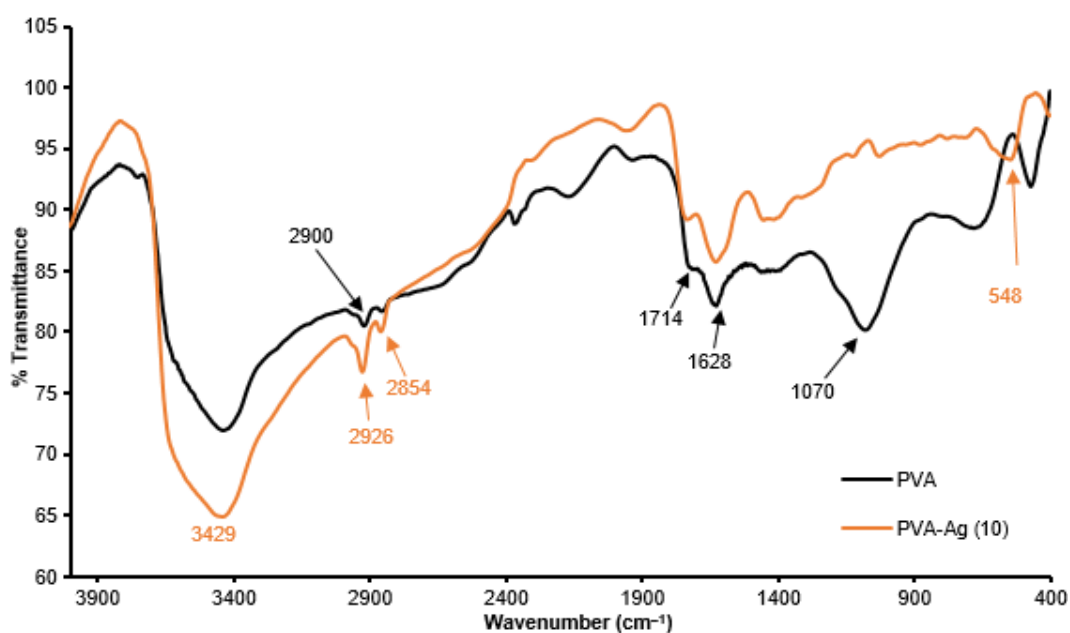


Fig 4. FTIR spectra of (a) PVA (b) PVA-Ag (10)

Ultraviolet-Visible Absorption Spectroscopy (UV-Vis)

The optical properties of PVA composite films were evaluated using UV-Visible spectroscopy. One of the important characteristics of food packaging applications is film transparency in terms of light transmittance (T%) [37]. Fig. 5 shows that pure PVA has a transparency of about 88%, which reflects its high crystallinity, whereas the transmittance of crosslinked PVA film was slightly decreased when compared to control PVA. On the contrary, the addition of AgNPs/MO noticeably has changed the transparency of the PVA films; there is about a 20% fall in the transparency of PVA-Ag (10). These results may be induced by the incident light loss from the light transmission, scattering, absorption, reflection, and refraction of the light when striking an interface while such a loss was increased especially at interfacial areas [38]. Nevertheless, AgNPs/MO incorporation conserved the transparency of PVA to some extent.

Thermal Gravimetric Analysis (TGA)

It is seen from Fig. 6 that PVA has a 7% weight loss at a range from 85 to 160 °C related to the desorbed water, another peak starts at 180 to 280 °C with weight loss of about 10% and the major weight loss of about 60% at temperature maxima around 350 °C. The former peak can

be assigned to the side chain of PVA, while the later peak can be related to a decomposition of the main chain of PVA [25]. After the incorporation of AgNPs/MO, the curves showed a relatively good thermal stability compared with the unmodified sheet with keeping the same behavior of the degradation. There is no great difference between the thermal behavior for PVA-Ag (2.5 and 10). The weight loss peak around 85 to 160 °C was about 5.6% related to the adsorbed water for PVA-Ag (10). For the second and third peaks, the weight loss reached 9 and 58.5% related to side chain and main chain degradation, respectively, of the composite film. These results indicate the good thermal stability of the composite film compared with the blank PVA film.

Mechanical Properties

As previously reported, the mechanical properties likely to be altered as metal nanoparticles are embedded in polymeric films [38]. Fig. 7 displayed that pure PVA has a tensile strength of 55 MPa and elongation at the break of about 222%. For composite sheets, there is no drastic change of the elongation at break when compared to the crosslinked films, whereas the tensile strength was decreased to 46 for both PVA-Ag (2.5 and 10). It was interesting to find out that the concentration of nanoparticle suspension has no great effect on mechanical

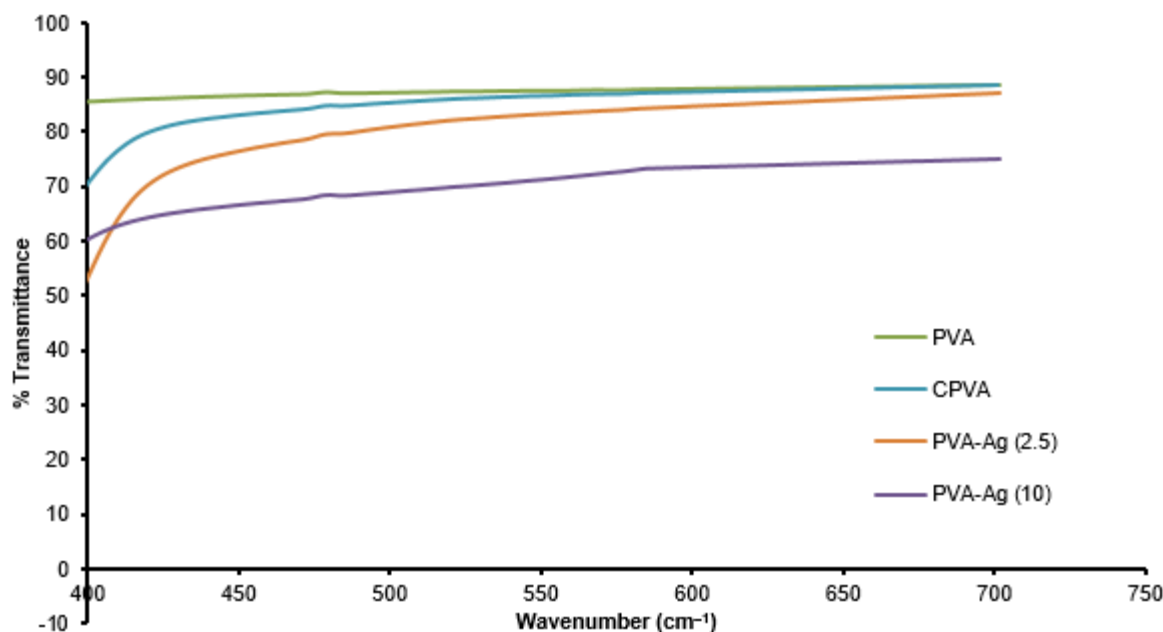


Fig 5. Optical properties of PVA composite films

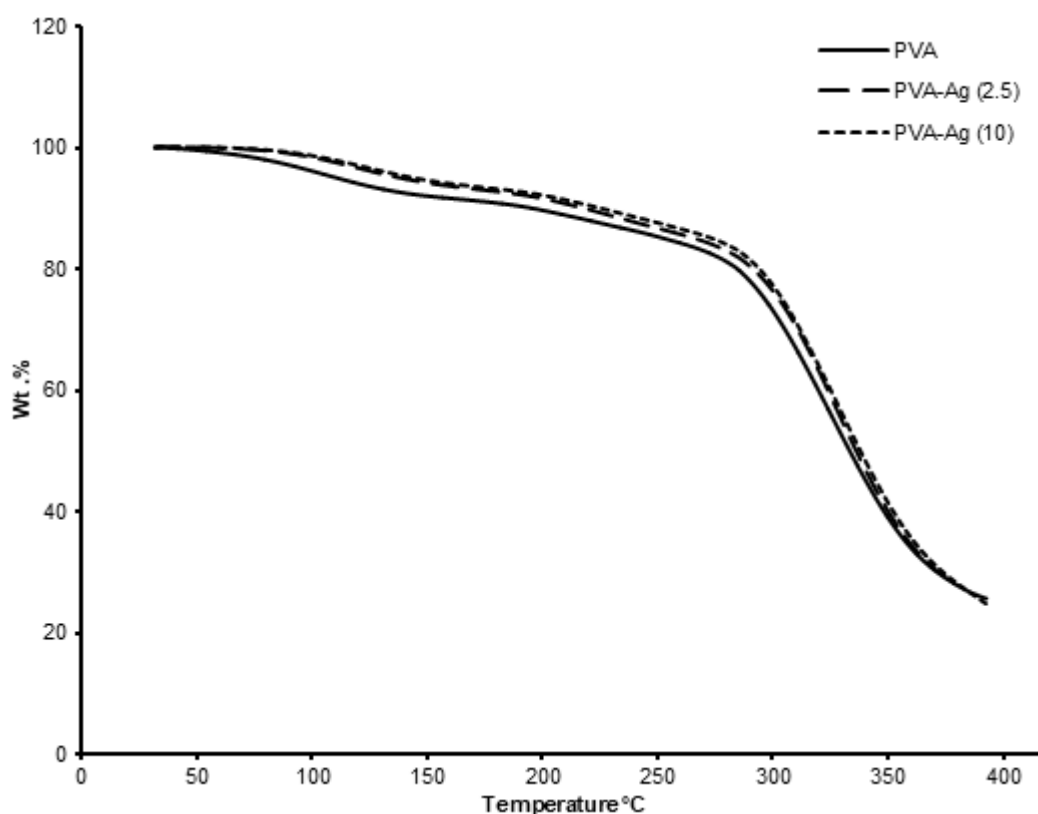


Fig 6. TGA of the prepared PVA sheets; PVA, PVA-Ag (2.5), and PVA-Ag (10)

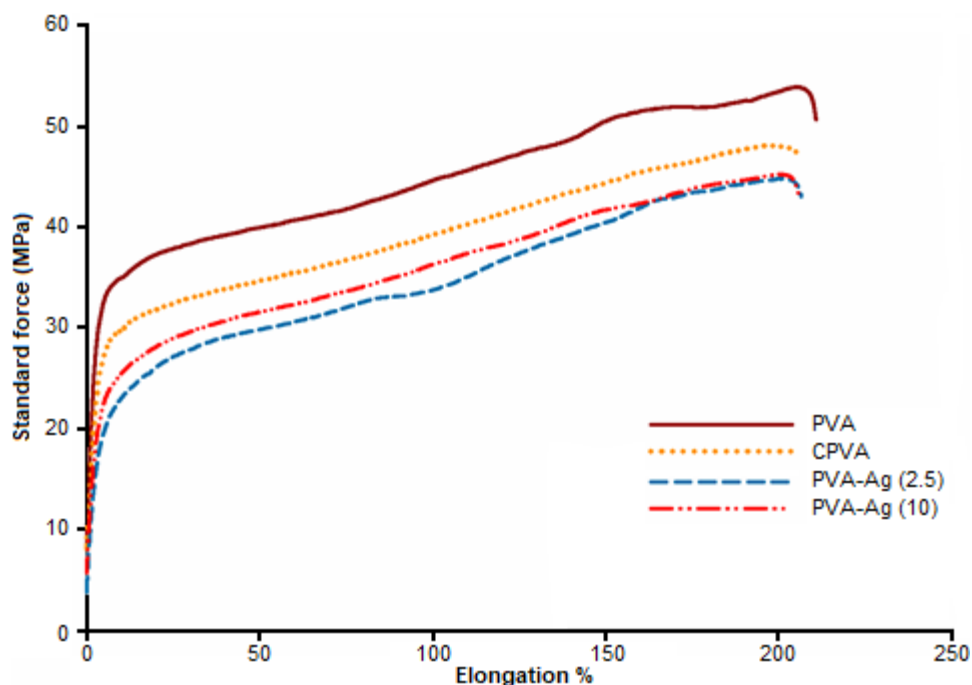


Fig 7. Tensile properties of (a)PVA, (b) CPVA, (c) CPVA-Ag (2.5) and (d) CPVA-Ag (10)

performance. This can be attributed to the reduction of PVA chain interaction due to the presence of AgNPs/MO

between the chains. However, the presence of the phenolic and reactive organic compounds in Moringa

extract can form hydrogen bonding between them and OH of PVA chains, so the decline in mechanical behavior is not so large. Also, the change in the crystallinity of PVA by incorporation of AgNPs/MO leads to a slight stiffness in the films.

Water Content

As most biopolymers have a high sensitivity to water, the study of the water content is an essential aspect, particularly concerning food packaging applications. However, it depends on the type of food and packaging materials. The stability of the packaging system still characterizes the capability of the packaging film to increase the food shelf life. Table 1 shows that the incorporation of AgNPs has no drastic change in the PVA ability to water retention, and there is no drastic change between PVA-Ag (2.5) and PVA-Ag (10).

Water Vapor Permeation

The film's ability to hinder the moisture from penetrating through is considered to be one of the most important characteristic features in food packaging materials as it is favorable to decrease the moisture transfer either from food or from the environment through the packaging films [2]. As shown from the data of Table 1, it is clear that the water vapor permeability rate (WVPR) had significantly decreased by adding AgNPs/MO, while there is no observed difference between the two ratios. These results indicate the improvement of the film to retard the vapor permeation and give an efficient property in food packaging applications.

Antibacterial Activity

The antibacterial properties of the composite films of PVA with AgNP/MO were assessed and demonstrated in Table 2. As shown in the table, all films showed antibacterial performance towards both Gram-positive and Gram-negative bacteria. The antibacterial of blank PVA film may be due to the presence of a trace of sulfuric acid during the preparation step that may unreacted and still present within the film. The antibacterial performance for the silver incorporated film (PVA Ag (10)) showed enhanced performance towards *E. coli* and

Table 1. Water content of nanocomposite PVA films and water vapor permeability rate

Sample	Water content %	WVPR (mg.mm/m ² hkPa)
PVA	-	-
CPVA	82.50397	1337.58
PVA-Ag (2.5)	81.65903	1261.01
PVA-Ag (10)	81.88466	1261.14

Table 2. Inhibition zone (mm) of PVA with and without AgNPs/MO

Film type	<i>E. coli</i>	<i>S. aureus</i>
PVA	12.4 ± 0.15	12.2 ± 0.18
PVA-Ag (10)	15.2 ± 0.20	14.8 ± 0.22

S. aureus and recorded the inhibition zone of 15.2 and 14.8 mm, respectively. The silver nanoparticle is well known for bactericidal action due to their enhanced reactivity resultant from their high surface/volume ratio and can enter the bacteria cell wall causing morphological alterations to the cell wall of bacteria and may result in a significant increase in its permeability and affect proper transport through the plasma membrane [39]. Silver nanoparticles have also been reported to release silver ions inside the bacterial cells and reacted with phosphorus and sulfur compounds producing their bactericidal activity [40].

CONCLUSION

The simple preparation of efficient and green nanocomposite films for active packaging was carried out. First, AgNPs were prepared with a distinguished particle size of 2–5 nm using local MO leaves extract as a reductive agent. Then, AgNPs were blended with a PVA solution and crosslinked with citric acid to form nanocomposite films. It was found upon thermal and mechanical testing that there is a clear enhancement in thermal stability with maintaining the flexibility of PVA. Further enhancement was recorded upon the addition of AgNPs/MO in the water content and water vapor permeability rate. The antimicrobial study showed a significant impact on the growth inhibition of Gram-negative *E. coli* and Gram-positive *S. aureus*.

■ REFERENCES

- [1] Mathew, S., Snigdha, S., Mathew, J., and Radhakrishnan, E.K., 2019, Biodegradable and active nanocomposite pouches reinforced with silver nanoparticles for improved packaging of chicken sausages, *Food Packag. Shelf Life*, 19, 155–166.
- [2] Sarwar, M.S., Niazi, M.B.K., Jahan, Z., Ahmad, T., and Hussain, A., 2018, Preparation and characterization of PVA/nanocellulose/Ag nanocomposite films for antimicrobial food packaging, *Carbohydr. Polym.*, 184, 453–464.
- [3] Garcia, C.V., Shin, G.H., and Kim, J.T., 2018, Metal oxide-based nanocomposites in food packaging: Applications, migration, and regulations, *Trends Food Sci. Technol.*, 82, 21–31.
- [4] Ragab, T.I.M., Nada, A.A., Ali, E.A., Shalaby, A.S.G., Soliman, A.A.F., Emam, M., and El Raey, M.A., 2019, Soft hydrogel based on modified chitosan containing *P. granatum* peel extract and its nano-forms: Multiparticulate study on chronic wounds treatment, *Int. J. Biol. Macromol.*, 135, 407–421.
- [5] El-Ghaffar, M.A.A., Elawady, M.M., Rabie, A.M., and Abdelhamid, A.E., 2020, Enhancing the RO performance of cellulose acetate membrane using chitosan nanoparticles, *J. Polym. Res.*, 27 (11), 337.
- [6] Kołodziejczak-Radzimska, A., and Jesionowski, T., 2014, Zinc oxide-from synthesis to application: A review, *Materials*, 7 (4), 2833–2881.
- [7] Newman, M.D., Stotland, M., and Ellis, J.I., 2009, The safety of nanosized particles in titanium dioxide-and zinc oxide-based sunscreens, *J. Am. Acad. Dermatol.*, 61 (4), 685–692.
- [8] Moodley, J.S., Krishna, S.B.N., Pillay, K., Sershen, and Govender, P., 2018, Green synthesis of silver nanoparticles from *Moringa oleifera* leaf extracts and its antimicrobial potential, *Adv. Nat. Sci.: Nanosci. Nanotechnol.*, 9 (1), 015011.
- [9] El-Shahat, M., Abdelhamid, A.E., and Abdelhameed, R.M., 2020, Capture of iodide from wastewater by effective adsorptive membrane synthesized from MIL-125-NH₂ and cross-linked chitosan, *Carbohydr. Polym.*, 231, 115742.
- [10] Abdelhamid, A.E., and Khalil, A.M., 2019, Polymeric membranes based on cellulose acetate loaded with candle soot nanoparticles for water desalination, *J. Macromol. Sci. Part A Pure Appl. Chem.*, 56 (2), 153–161.
- [11] Elhalawany, N., Wassel, A.R., Abdelhamid, A.E., Elfadl, A.A., and Nouh, S., 2020, Novel hyper branched polyaniline nanocomposites for gamma radiation dosimetry, *J. Mater. Sci. - Mater. Electron.*, 31 (8), 5914–5925.
- [12] Elhalawany, N., El-Naggar, M.E., Elsayed, A., Wassel, A.R., El-Aref, A.T., and Abd Elghaffar, M.A., 2020, Polyaniline/zinc/aluminum nanocomposites for multifunctional smart cotton fabrics, *Mater. Chem. Phys.*, 249, 123210.
- [13] Thakkar, K.N., Mhatre, S.S., and Parikh, R.Y., 2010, Biological synthesis of metallic nanoparticles, *Nanomed. Nanotechnol. Biol. Med.*, 6 (2), 257–262.
- [14] Ahmad, N., Sharma, S., Alam, M.K., Singh, V.N., Shamsi, S.F., Mehta, B.R., and Fatma, A., 2010, Rapid synthesis of silver nanoparticles using dried medicinal plant of basil, *Colloids Surf., B*, 81 (1), 81–86.
- [15] Yallappa, S., Manjanna, J., Peethambar, S.K., Rajeshwara, A.N., and Satyanarayan, N.D., 2013, Green synthesis of silver nanoparticles using *Acacia farnesiana* (Sweet Acacia) seed extract under microwave irradiation and their biological assessment, *J. Cluster Sci.*, 24 (4), 1081–1092.
- [16] Siddhuraju, P., and Becker, K., 2003, Antioxidant properties of various solvent extracts of total phenolic constituents from three different agroclimatic origins of drumstick tree (*Moringa oleifera* Lam.) leaves, *J. Agric. Food Chem.*, 51 (8), 2144–2155.
- [17] Ju, A., Baek, S.K., Kim, S., and Song, K.B., 2019, Development of an antioxidative packaging film based on khorasan wheat starch containing moringa leaf extract, *Food Science Biotechnol.*, 28 (4), 1057–1063.
- [18] El-Sayed, A.A., Amr, A., Kamel, O.M.H.M., El-Saidi, M.M.T., and Abdelhamid, A.E., 2020,

- Eco-friendly fabric modification based on AgNPs@Moringa for mosquito repellent applications, *Cellulose*, 27 (14), 8429–8442.
- [19] Ali, E.A., Eweis, M., Elkholy, S., Ismail, M.N., and Elsabee, M., 2018, The antimicrobial behavior of polyelectrolyte chitosan-styrene maleic anhydride nano composites, *Macromol. Res.*, 26 (5), 418–425.
- [20] Al-Moghazy, M., Mahmoud, M., and Nada, A.A., 2020, Fabrication of cellulose-based adhesive composite as an active packaging material to extend the shelf life of cheese, *Int. J. Biol. Macromol.*, 160, 264–275.
- [21] Tanase, E.E., Popa, E.M., Rapa, M., Popa, O., and Popa, I.V., 2016, Biodegradation study of some food packaging biopolymers based on PVA, *Bull. Univ. Agric. Sci. Vet. Med. Cluj-Napoca*, 73 (1), 11948.
- [22] Liu, B., Xu, H., Zhao, H., Liu, W., Zhao, L., and Li, Y., 2017, Preparation and characterization of intelligent starch/PVA films for simultaneous colorimetric indication and antimicrobial activity for food packaging applications, *Carbohydr. Polym.*, 157, 842–849.
- [23] Musetti, A., Paderni, K., Fabbri, P., Pulvirenti, A., Al-Moghazy, M., and Fava, P., 2014, Poly(vinyl alcohol)-based film potentially suitable for antimicrobial packaging applications, *J. Food Sci.*, 79 (4), E557–E582.
- [24] Bindhu, M.R., Umadevi, M., Esmail, G.A., Al-Dhabi, N.A., and Arasu, M.V., 2020, Green synthesis and characterization of silver nanoparticles from *Moringa oleifera* flower and assessment of antimicrobial and sensing properties, *J. Photochem. Photobiol., B*, 205, 111836.
- [25] Prasad, T.N.V.K.V., and Elumalai, E.K., 2011, Biofabrication of Ag nanoparticles using *Moringa oleifera* leaf extract and their antimicrobial activity, *Asian Pac. J. Trop. Biomed.*, 1 (6), 439–442.
- [26] Abdullah, Z.W., Dong, Y., Han, N., and Liu, S., 2019, Water and gas barrier properties of polyvinyl alcohol (PVA)/starch (ST)/glycerol (GL)/halloysite nanotube (HNT) bionanocomposite films: Experimental characterisation and modelling approach, *Composites, Part B*, 174, 107033.
- [27] Marrez, D.A., Abdelhamid, A.E., and Darwesh, O.M., 2019, Eco-friendly cellulose acetate green synthesized silver nano-composite as antibacterial packaging system for food safety, *Food Packag. Shelf Life*, 20, 100302.
- [28] Zidan, T.A., Abdelhamid, A.E., and Zaki, E.G., 2020, N-Aminorhodanine modified chitosan hydrogel for antibacterial and copper ions removal from aqueous solutions, *Int. J. Biol. Macromol.*, 158, 32–42.
- [29] Bennett, R.N., Mellon, F.A., Foidl, N., Pratt, J.H., Dupont, M.S., and Perkins, L., 2003, Profiling glucosinolates and phenolics in vegetative and reproductive tissues of the multi-purpose trees *Moringa oleifera* L. (Horseradish tree) and *Moringa stenopetala* L., *J. Agric. Food Chem.*, 51 (12), 3546–3553.
- [30] Fahey, J.W., Zalcmann, A.T., and Talalay, P., 2001, The chemical diversity and distribution of glucosinolates and isothiocyanates among plants, *Phytochemistry*, 56 (1), 5–51.
- [31] El-Bisi, M.K., El-Rafie, H.M., El-Rafie, M.H., and Hebeish, A., 2013, Honey bee for eco-friendly green synthesis of silver nanoparticles and application to cotton textile, *Egypt. J. Chem.*, 56 (3), 187–198.
- [32] Pinoni, S.A., and López Mañanes, A.A., 2009, Na⁺ ATPase activities in chela muscle of the euryhaline crab *Neohelice granulata*: Differential response to environmental salinity, *J. Exp. Mar. Biol. Ecol.*, 372 (1-2), 91–97.
- [33] Sathyavathi, R., Krishna, M.B.M., and Rao, D.N., 2011, Biosynthesis of silver nanoparticles using *Moringa oleifera* leaf extract and its application to optical limiting, *J. Nanosci. Nanotechnol.*, 11 (3), 2031–2035.
- [34] Shakir, M.A., Yhaya, M.F., and Ahmad, M.I., 2017, The effect of crosslinking fibers with polyvinyl alcohol using citric acid the effect of crosslinking fibers with polyvinyl alcohol using citric acid, *Imp. J. Interdiscip. Res.*, 3 (4), 758–764.
- [35] Moghazy, R.M., Labena, A., Husien, S., Mansor, E.S., and Abdelhamid, A.E., 2020, Neoteric approach for efficient eco-friendly dye removal and

- recovery using algal-polymer biosorbent sheets: Characterization, factorial design, equilibrium and kinetics, *Int. J. Biol. Macromol.*, 157, 494–509.
- [36] Mansor, E.S., Labena, A., Moghazy, R.M., and Abdelhamid, A.E., 2020, Advanced eco-friendly and adsorptive membranes based on *Sargassum dentifolium* for heavy metals removal, recovery, and reuse, *J. Water Process Eng.*, 37, 101424.
- [37] Abdullah, Z.W., and Dong, Y., 2019, Biodegradable and water resistant poly(vinyl) alcohol (PVA)/starch (ST)/glycerol (GL)/halloysite nanotube (HNT) nanocomposite films for sustainable food packaging, *Front. Mater.*, 6, 58.
- [38] Cai, J., Chen, J., Zhang, Q., Lei, M., He, J., Xiao, A., Ma, C., Li, S., and Xiong, H., 2016, Well-aligned cellulose nanofiber-reinforced polyvinyl alcohol composite film: Mechanical and optical properties, *Carbohydr. Polym.*, 140, 238–245.
- [39] Morones, J.R., Elechiguerra, J.L., Camacho, A., Holt, K., Kouri, J.B., Ramírez, J.T., and Yacaman, M., 2005, The bactericidal effect of silver nanoparticles, *Nanotechnology*, 16 (10), 2346–2353.
- [40] Cardozo, V.F., Oliveira, A.G., Nishio, E.K., Perugini, M.R.E., Andrade, C.G.T.J., Silveira, W.D., Durán, N., Andrade, G., Kobayashi, R.K.T., and Nakazato, G., 2013, Antibacterial activity of extracellular compounds produced by a *Pseudomonas* strain against methicillin-resistant *Staphylococcus aureus* (MRSA) strains, *Ann. Clin. Microbiol. Antimicrob.*, 12 (1), 12.